6852 *J. Am. Chem. Soc.* **1986**, *108*, 6852-6857

^{13}C NMR Studies of Chemical-Shielding Tensors and Molecular Motion in Meldrum's Acid in the Solid State

K. Takegoshi and C. A. McDowell*

Contribution from the Department of Chemistry, University of British Columbia, 2036 Main Mall, Vancouver, British Columbia V6T 1Y6, Canada. *Received February 18, 1986*

Abstract: The chemical-shielding tensors of the ^{13}C nuclei in Meldrum's acid were determined by employing high-resolution solid-state NMR techniques. The tensors of two ester carbon nuclei in Meldrum's acid are compared with each other and also with those of the carboxyl carbon nuclei in Malonic acid. Differences in the tensors of the two ester carbon nuclei are attributed to the different intermolecular C=O---H—C interactions reported in an X-ray crystallographic study. The application of a one-dimensional exchange NMR technique enabled us to determine the rate of the motional process involving an interchange of the location of the two ester carbon nuclei in the crystal lattice. The dynamic process is postulated to be ring inversion plus a rotation of the molecule by 180°, and it thus involves the alternation of the intermolecular C=O---H—C interactions in the crystal lattice. The activation energy for this molecular rotation process was determined to be 91.4 ± 4.6 kJ/mol.

Meldrum's acid (2,2-dimethyl-1,3-dioxane-4,6-dione, **1**) is a compound of versatile synthetic use because of its susceptibilities for both nucleo- and electrophilic reactions.[1] These susceptibilities arise from a facile loss of one of the two hydrogen nuclei bonded to the CH_2 carbon nucleus (C5) and an acidity of **1** (pK 4.83–4.93, ref 2) which is comparable to that of acetic acid (pK 4.76). This strong acidity and the fact that dimedone (5,5-dimethyl-1,3-cyclohexanedione, **2**), which is a weaker acid (p*K* 5.2, ref 3) having a similar 1,3-diketo formula, enolizes in the solid state[4] initially influenced us to think that **1** is in the enol form in the solid state. However, this naive expectation is incorrect. Meldrum's acid exists in the diketo form both in the solid state and in solution. Recent X-ray studies[5,6] of **1** clearly show that it has the diketo form with a boat conformation in the crystalline state. Moreover, that work confirmed[5] the existence of relatively short intermolecular C=O---H—C5 distances. It seemed interesting to investigate the chemical nature of **1** in the solid state by using NMR techniques.

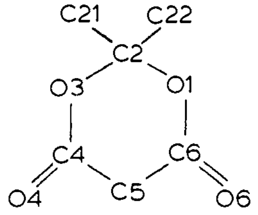

(1)

Recent developments in high-resolution solid-state NMR techniques permit us not only to investigate the local electronic structure around a nucleus by determining chemical-shielding tensors[7] but also to study slow molecular motion occurring in the solid state.[8] In our investigation of the effects of hydrogen bonding on the chemical-shielding tensors in 1,3-keto–enol carbon nuclei,[9] we have determined the ^{13}C shielding tensors in **1**. The tensors of the ester carbon nuclei in **1** (C4 and C6) are compared with those of the corresponding carboxyl carbon nuclei in malonic acid (**3**),[10] and the differences are found to be most prominent for the tensor component oriented along the C=O bond direction. Further, the observed differences in the shielding tensors in the two ester carbon nuclei in **1** (C4 and C6) are attributed to the differences in the intermolecular C=O---H—C interactions in the crystal. Finally, application of a one-dimensional exchange NMR technique[11] at various temperatures reveals a slow molecular motion involving a spatial alternation of the intermolecular C=O---H—C interactions in **1**, and the associated activation parameters were determined.

Experimental Section

Material. Meldrum's acid was purchased from the Aldrich Chemical Co., and the crystals were grown from a saturated benzene–dichloromethane 1:1 solution by slow evaporation at room temperature (293 K). The crystals are orthorhombic, belonging to the space group *Pbca* with unit cell dimensions a = 6.055 (6.048) Å, b = 13.746 (13.721) Å, and c = 16.629 (16.592) Å. The former values are from ref 5, while the values in parentheses are from ref 6. Single crystals of dimensions 2 × 2 × 5 mm were mounted on an accurate goniometer in the probe.[12]

Table I. Isotropic ^{13}C Chemical Shift Values for Carbon Nuclei in **1**[a]

carbon nucleus	in solids		in solution	
	single crystal	CP-MAS	ref 23a	ref 23b
C2	107.8	107.4	106.0	106.4
C4	166.6	166.6	163.0	164.0
C5	38.9	39.3	35.4	36.8
C6	165.5	164.3	163.0	164.0
C21	26.2	25.8	26.4	27.5
C22	29.9	29.6	26.4	27.5

[a] The chemical shift values are in ppm from Me_4Si as a standard.

^{13}C NMR Measurements in Solids. The ^{13}C NMR measurements were made with a Brucker CXP200 FT NMR spectrometer operating at 200.05 MHz for ^{1}H and 50.3 MHz for ^{13}C. High-resolution solid-state ^{13}C NMR spectra were obtained by using the combined techniques[13] of high-power proton decoupling[14] and cross-polarization[15] (CP) and with[16] or without magic angle spinning[17] (the MAS). The radio frequency field strength for both

---

* Author to whom correspondence should be addressed.

(1) For a review, see: McNab, H. *Chem. Soc. Rev.* **1978**, *7*, 345–358.

(2) (a) Pihlaja, K.; Seilo, M. *Acta Chem. Scand.* **1968**, *22*, 3053–3062. (b) Pihlaja, K.; Seilo, M. *Acta Chem. Scand.* **1969**, *23*, 3003–3010.

(3) Schwarzenbach, G.; Felder, E. *Helv. Chim. Acta* **1944**, *27*, 1701–1711.

(4) (a) Semmingsen, D. *Acta Chem. Scand.* **1974**, *B28*, 169–174. (b) Singh, I.; Calvo, C. *Can. J. Chem.* **1975**, *53*, 1046–1050.

(5) Pfluger, C. E.; Boyle, P. D. *J. Chem. Soc., Perkin Trans. 2* **1985**, 1547–1549.

(6) Evans, S. V., private communication.

(7) For a review, see: Veeman, W. S. *Progr. NMR Spectrosc.* **1984**, *16*, 193–235.

(8) Szeverenyi, N. M.; Bax, A.; Maciel, G. E. *J. Am. Chem. Soc.* **1983**, *105*, 2579–2582.

(9) (a) Takegoshi, K.; Naito, A.; McDowell, C. A. *J. Magn. Reson.* **1985**, 65, 34–42. (b) Takegoshi, K.; McDowell, C. A. *Chem. Phys. Lett.* **1986**, *123*, 159–163.

(10) Tegenfeldt, J.; Feucht, H.; Rushitzka, G.; Haeberlen, U. *J. Magn. Reson* **1980**, *39*, 509–520.

(11) Connor, C.; Naito, A.; Takegoshi, K.; McDowell, C. A. *Chem. Phys. Lett.* **1985**, *113*. 123–128.

(12) Naito, A.; McDowell, C. A. *J. Chem. Phys.* **1984**, *81*, 4795–4803.

(13) Pines, A.; Gibby, M. G.; Waugh, J. S. *J. Chem. Phys.* **1973**, *59*, 569–590.

(14) Sarles, L. R.; Cotts, R. M. *Phys. Rev.* **1958**, *111*, 853–859.

(15) Hartmann, S. R.; Hahn, E. L. *Phys. Rev.* **1962**, *128*, 2042–2053.

(16) Schaefer, J.; Stejskal, E. O. *J. Am. Chem. Soc.* **1976**, *98*, 1030–1032.

0002-7863/86/1508-6852$01.50/0

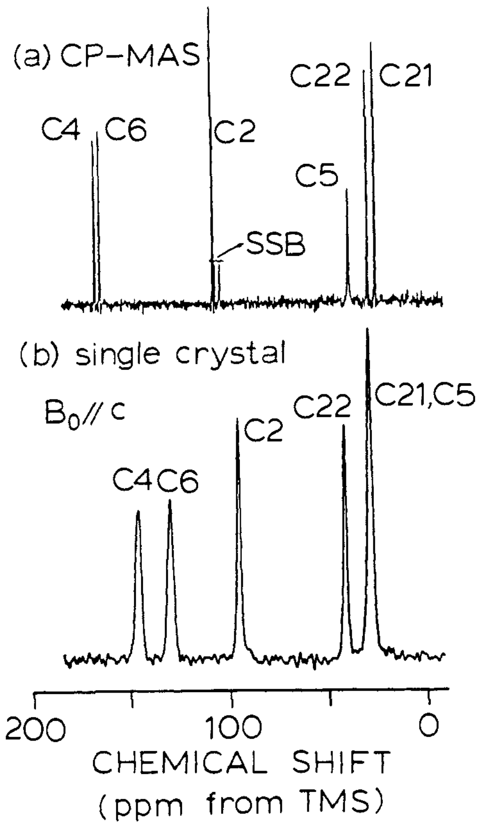

Figure 1. ^{13}C solid-state NMR spectra of Meldrum's acid: (a) CP-MAS, (b) single crystal when the static magnetic field is pointed in the direction of the crystallographic *c* axis.

^1H and ^{13}C was about 42 kHz. An Andrew-Beams type Kel-F rotor was used for the MAS at a spinning frequency of approximately 3.0 kHz. The setting of the magic angle was monitored by the ^{79}Br NMR spectrum of KBr incorporated in the rotor.[18] FID signals were accumulated 20–50 times with a contact time of 2 ms and a repetition time of 2 s. To avoid unnecessary interferences caused by off-resonance proton decoupling, the ^1H decoupling frequency was chosen to be 3 ppm from Me_4Si.[19] The ^{13}C chemical shifts were calibrated in ppm relative to Me_4Si as described previously.[9] No attempts were made to correct bulk susceptibility effects, because these are expected to be small.[20] The chemical-shielding tensors were determined at room temperature. The 1D-exchange NMR technique,[8,11] employing the conventional pulse sequence applied for the 2D-exchange NMR experiments of a dilute spin in solids,[21] was applied to study molecular motion in solid Meldrum's acid. Variable-temperature measurements to determine the activation parameters involved in the molecular motions observed by the 1D-exchange NMR technique were accomplished by using a Brucker B-VT-1000 temperature controller.

Results and Discussion

Isotropic Chemical Shifts. The ^{13}C signals in the CP–MAS spectrum (Figure 1a) were assigned by reference to the isotropic ^{13}C chemical shifts obtained from the complete chemical-shielding tensors ($\bar{\sigma} = (\sigma_{11} + \sigma_{22} + \sigma_{33})/3$, vide infra[22]) and are listed in Table I together with those measured in solution.[23] The agreement between the isotropic chemical shift values obtained from the CP–MAS experiment and the single crystal experiments is satisfactory. There is a direct correspondence between the isotropic chemical shifts in the solid state and those in solution; however, slight differences, involving the splitting of signals consisting of a single peak in solution into two peaks in the solid state, are noticable. These differences in the chemical shifts are generally attributed to so-called solid-state effects, such as, crystal packing effects, effects of freezing-in of molecular conformation, intermolecular hydrogen-bonding effects, etc. Particularly, it is interesting to note that, although molecule **1** seems to have C_{2v} symmetry, the two ester carbon nuclei have different isotropic chemical shifts in the solid state (166.6 ppm for C4 and 164.3 ppm for C6). This will be examined later by comparing the complete tensors for the C4 and C6 carbon nuclei.

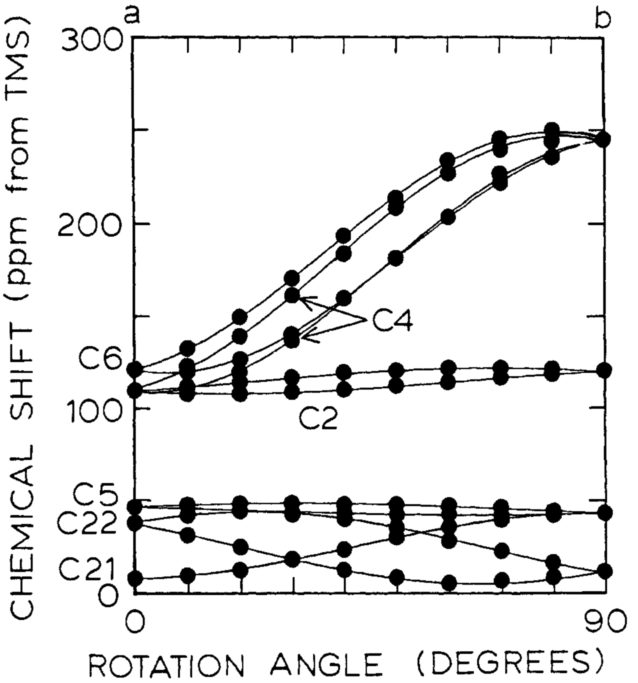

Figure 2. Angular dependence of the ^{13}C NMR lines for the *ab* plane for a single crystal of Meldrum's acid.

Chemical Shielding Tensors. (a) Determination of the ^{13}C Shielding Tensors. The ^{13}C NMR spectra for a single crystal of **1** were obtained as a function of the angle of rotation about the three orthogonal crystallographic axes *a*, *b*, and *c*. Figure 1b shows the spectrum obtained when the static magnetic field is directed along the crystallographic *c* axis, and Figure 2 shows the orientation dependence of the ^{13}C NMR line positions when the static magnetic field is in the crystallographic *ab* plane. The orientational dependence of the chemical shifts, $\sigma(\theta,\phi)$, can be written as[7]

$$\sigma(\theta,\phi) = \sigma_{kk} \sin^2\theta \cos^2\phi + \sigma_{ii} \sin^2\theta \sin^2\phi + \sigma_{jj} \cos^2\theta + \sigma_{ik} \sin^2\theta \sin 2\phi + \sigma_{jk} \sin 2\theta \cos\phi + \sigma_{ji} \sin 2\theta \sin\phi \quad (1)$$

where the *j* axis is at an angle θ to the static magnetic field, and the angle ϕ is an azimuthal angle from the *k* axis defining the orientation of the magnetic field in the orthogonal *kij* axes system. When the magnetic field is in the *jk* plane ($\phi = 0$), the orientational dependence of the chemical shifts is written as

$$\sigma(\theta) = \sigma_{jj} \cos^2\theta + \sigma_{jk} \sin 2\theta + \sigma_{kk} \sin^2\theta \quad (2)$$

and the experimental values of the orientational dependence of

---

[17] Andrew, E. R. *MTP Int. Rev. Sci. Phys. Chem. Ser. 2* **1975**, *4*, 173–208.

[18] Frye, J. S.; Maciel, G. E. *J. Magn. Reson.* **1982**, *48*, 125–131.

[19] Takegoshi, K.; McDowell, C. A. *J. Magn. Reson.* **1986**, *66*, 14–31.

[20] (a) Osborn, J. A. *Phys. Rev.* **1945**, *67*, 351–357. (b) Appleman, B. R.; Dailey, B. P. *Adv. Magn. Reson.* **1974**, *7*, 231–320. (c) VanderHart, D. L.; Earl, W. L.; Garroway, A. N. *J. Magn. Reson.* **1981**, *44*, 361–401.

[21] Szeverenyi, N. M.; Sullivan, M. J.; Maciel, G. E. *J. Magn. Reson.* **1982**, *47*, 462–475.

[22] It might be appropriate to use δ instead of σ in this study; however, the review article (ref 7) and also other recent articles prefer to use σ_{ij} rather than δ_{ij}.

[23] (a) Billman, J. H.; Sojka, S. A.; Taylor, P. R. *J. Chem. Soc., Perkin Trans. 2* **1972**, 2034–2035. The chemical shifts listed in this reference were recalibrated by taking the chemical shift of carbon disulfide as 192.8 ppm from Me_4Si. (Martin, M. L.; Martin, D. J.; Delpuech, J.-J. *Practical NMR Spectroscopy*; Heyden: London, 1980, Table 5.3). (b) Äyräs, P. *Acta Chem. Scand.* **1976**, *B30*, 957–962.

Table II. Principal Values and Direction Cosines of the ^{13}C Chemical Shielding Tensors in Meldrum's Acid (**1**) Relative to the Crystallographic Axes (*abc*) and the Molecular Fixed Axes (*XYZ*)[a,b]

carbon nucleus		principal values	direction cosines with respect to						l_i ($i = 1 \sim 3$)
			a	*b*	*c*	*X*	*Y*	*Z*	
C2	σ_{33}	91.2	0.4323	−0.1029	0.8958	−0.0814	0.9945	−0.0655	C2
	σ_{22}	110.6	0.7971	−0.4210	−0.4330	−0.9032	−0.0458	0.4269	O[c]
	σ_{11}	121.6	−0.4217	−0.9012	0.0999	−0.4215	−0.0940	−0.9019	O3
C4	σ_{33}	107.3	−0.9836	−0.0114	0.1798	0.0655	0.0525	0.9964	C4
	σ_{22}	138.9	−0.1695	−0.2087	−0.9447	−0.9844	0.1666	0.0560	O4
	σ_{11}	253.5	0.0613	−0.9597	0.2741	−0.1631	−0.9846	0.0626	C5
C5	σ_{33}	23.2	0.4081	−0.0286	0.9125	−0.0495	−0.9976	0.0478	C5
	σ_{22}	42.1	−0.2409	−0.9675	0.0774	−0.9957	0.0456	−0.0814	H[d]
	σ_{11}	51.4	0.8806	−0.2514	−0.4017	0.0791	−0.0516	−0.9955	C6
C6	σ_{33}	110.6	−0.8053	−0.0128	0.5927	0.1003	0.0118	−0.9949	C6
	σ_{22}	128.3	−0.5682	0.3018	−0.7655	0.9878	−0.1205	0.0982	O6
	σ_{11}	257.5	−0.1691	−0.9533	−0.2503	−0.1188	−0.9926	−0.0238	C5
C21	σ_{33}	2.4	−0.9141	0.0241	0.4048	0.9987	0.0084	0.0500	C21
	σ_{22}	33.0	−0.3921	0.2020	−0.8975	−0.0262	−0.7585	0.6512	C2
	σ_{11}	43.1	0.1034	0.9791	0.1751	−0.0435	0.6516	0.7573	O3
C22	σ_{33}	3.7	−0.3773	−0.9099	0.1724	−0.9984	−0.0152	−0.0540	C22
	σ_{22}	36.8	0.6797	−0.1456	0.7189	−0.0517	0.6224	0.7810	C2
	σ_{11}	49.3	0.6290	−0.3884	−0.6734	−0.0217	−0.7825	0.6222	O3

[a] *XYZ* is defined by the three atoms listed in Table II as l_1, l_2, and l_3 as follows: l_1 is taken to be origin, the *X* axis is along the direction of l_1–l_2, and the *XY* plane is spanned by l_1–l_2–l_3. [b] The chemical shift values are given as ppm from Me_4Si as a standard. The standard deviation for the principal values is ±0.6 ppm. [c] Average of two ester oxygen atoms. [d] Average of two bonded hydrogen atoms.

the chemical shifts were least-squares fitted to eq 2, taking σ_{jj}, σ_{jk}, and σ_{kk} as adjustable parameters, where the subscripts *i*, *j*, and *k* represent the crystallographic axes *a*, *b*, and *c*.

The crystallographic symmetry *Pbca* means that there are two magnetically nonequivalent molecules in a unit cell when the static magnetic field is in the crystallographic *ab*, *bc*, and *ca* planes. Therefore, eight tensors can be assigned to a particular carbon nucleus in **1**. Because there are two ester carbon nuclei, and the assignments of the chemical shifts for them are not known a priori, there are 16 possible tensors for each ester carbon nucleus in **1**. Similarly, there are 16 possibilities for each methyl carbon nucleus in **1**. Fortunately, the doublet lines for some carbon nuclei accidentally become one unresolved line when the static magnetic field is in the *ab* and *bc* planes thus reducing the number of possible tensors. To choose the four correct tensors out of eight found experimentally, a general plane experiment was performed by rotating the static magnetic field in the crystallographic (021) plane. Four tensors could be chosen by comparing the experimental chemical shift values with the values calculated for the eight possible tensors from eq 1. Further, to choose one tensor out of four for a particular carbon in a molecular reference frame, we assumed that one of the tensors should reasonably reflect the local molecular configuration around the carbon nucleus concerned. For the quaternary and methylene carbon nuclei having approximately C_{2v} local structures, one set of the principal axis system of the ^{13}C shielding tensors of the carbon nucleus concerned was found to be parallel to the C_{2v} local symmetry axis system. For the methyl carbon nucleus, the σ_{33} axis of one of the ^{13}C shielding tensors was found to be collinear with the C–CH_3 bond direction. In the case of the ester carbon nucleus, we found the σ_{33} axes of some tensors were perpendicular to the plane spanned by the O=C—O nuclei. The principal values of the chemical shielding tensors and their direction cosines with respect to the crystallographic axes, *a*, *b*, and *c*, and the molecular fixed axes are collated in Table II. An ORTEP drawing of the ^{13}C shielding tensors is represented in Figure 3.

(b) Methyl Carbons (C21 and C22). The σ_{33} axes of the chemical-shielding tensors for both the C21 and the C22 carbon nuclei are almost parallel to those of the corresponding C–CH_3 bond to within ±3°, showing good agreement with what is observed[9] for the methyl carbons in **2**. Moreover, the isotropic chemical shifts for the methyl carbons also show good correspondence in **1** and **2**; the isotropic chemical shifts for the axial methyl carbon nuclei in **1** and **2** (C21 in **1** and C8 in **2**) are around 26 ppm, while those for the equatorial methyl carbon nuclei in **1** and **2** (C22 in **1** and C7 in **2**) are around 31 ppm.[24] Since the molecular configurations of **1** and **2** are frozen in the solid state, we could observe two distinct chemical shift tensors for the axial and the equatorial methyl carbon nuclei. In solution, a fast overall molecular motion involving a ring inversion[25] interchanging the spatial positions of the axial and the equatorial methyl groups would average not only the anisotropy of the chemical shielding but also any difference between the axial and the equatorial methyl groups.

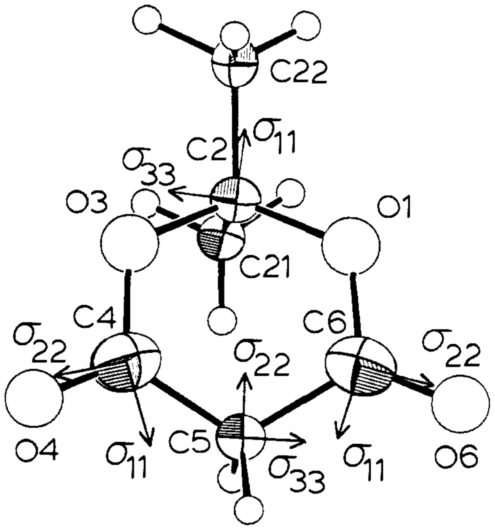

Figure 3. An ORTEP drawing showing the orientation of the principal values of the ^{13}C chemical shielding tensors for Meldrum's acid, viewing along the direction perpendicular to the C4–C5–C6 plane.

(c) Quaternary Carbon (C2). Studies of the shielding tensors of this type of carbon nucleus bonding two ester oxygen nuclei have not been reported. Thus we shall compare our result for the C2 with the sheilding tensor for the anomeric carbon nucleus (C1) in α-methylglucopyranoside (**4**) determined recently by our group.[26] Each σ_{11} axis in the shielding tensors for both carbon

---

(24) Imashiro, F.; Maeda, S.; Takegoshi, K.; Terao, T.; Saika, A. *Chem. Phys. Lett.* **1982**, *92*, 642–645.

(25) Anet, F. A. L., *Top. Current Chem.* **1974**, *45*, 169–220.

Table III. Comparison between the Principal Values of the ^{13}C Chemical-Shielding Tensors of the Ester Carbon Nuclei in **1** and the Carboxyl Carbon Nuclei in **3** (ref 10)[a]

Meldrum's acid			malonic acid		
σ_{11}	σ_{22}	σ_{33}	σ_{11}	σ_{22}	σ_{33}
253.5	138.9	107.3	244.0	179.0	108.5
257.5	128.3	110.6	248.0	174.5	111.0

[a] The chemical shift values are in ppm from Me_4Si as a standard. The chemical shift values in ref 10 were recalibrated by taking the chemical shift of liquid benzene as 128.5 ppm from Me_4Si.

nuclei (C2 in **1** and C1 in **4**) is found to lie approximately perpendicular to the plane spanned by the corresponding O–C–O nuclei. The other two principal axes are in the O–C–O plane. In **1**, the σ_{22} axis for the C2 carbon is nearest to the direction of the bisector of the angle between the two oxygen nuclei, reflecting the approximate C_2 symmetry of the C2 moiety.[27] In **4**, the other two principal axes in the O–C–O plane do not show such a close relation with any part of the molecular environment.[26]

(d) Methylene Carbon (C5). The orientation of the principal axes of the shielding tensor of the methylene carbon nucleus (C5) is typical for the CH_2 moiety having approximately C_{2v} symmetry; the σ_{22} axis lies close to the bisector of the angle between the two CH_2 protons, and the σ_{11} axis is almost perpendicular to the plane defined by C6–C5–H*, where H* denotes the average position of the two CH_2 protons.

(e) Ester Carbon (C4 and C6). A study of the shielding tensor of the ester carbon in dimethyl oxalate shows that the σ_{22} axis lies approximately along the C=O bond.[28] Similarly in **1**, each σ_{22} axis of the shielding tensors of the two ester carbon nuclei is, within ±10°, parallel to the corresponding C=O bond. Further, each σ_{33} axis is, within ±6°, perpendicular to the corresponding plane spanned by the C5—C=O nuclei. The orientations of the principal axes of the ester carbon nuclei in **1** are very similar to those of the carboxyl carbon nuclei in malonic acid[10] (**3**); however, the magnitudes of the tensor components are significantly different, particularly those along the C=O bond (σ_{22}), and there is a large upfield shift (~40 ppm) of the tensor component along the C=O bond in **1** as compared to that in **3** (Table III). In solution NMR, it has been pointed out that the chemical shift of the ester carbon nucleus appears upfield compared to that of the corresponding carboxylic carbon nucleus.[29] This upfield shift in the isotropic chemical shift can be attributed mainly to the upfield shift of the component of the chemical-shielding tensor of an ester carbon nucleus which lies along the C=O bond.

Interestingly, the magnitudes of the tensor component along the C=O bond characterize the chemical differences not only between the carboxyl carbons in **3** and the ester carbons in **1** but also between the two ester carbons in **1**. An appreciable difference (~ 10 ppm) between the magnitudes of the tensor component along the C=O bond (σ_{22}) of the C4 and C6 carbon nuclei in **1** is noteworthy. The *intramolecular* local configurations around the C4 and the C6 carbon nuclei in **1** are collated in Table IV and are essentially identical within ±1° in angle and ±0.01 Å in bond length.[5,6] This approximately C_{2v} symmetry within the molecule leads one to expect similar chemical-shielding tensors for the C4 and C6 carbon nuclei, therefore the origin of the difference in their shielding tensors can be mainly attributed to *intermolecular* effects. Pfluger and Boyle[5] showed the existence of relatively short *intermolecular* C=O- - -H—C distances in this compound. Furthermore, the configurations found in the intermolecular C4=O4- - -H′(equatorial)—C5′ approach are appreciably different from those found in the intermolecular C6=O6- - -H″(axitial)—C5″ approach (Table IV), where the primed H′, C5′ and the double primed H″, C5″ nuclei belong to molecules related by the transformations of $^1/_2 + x,y,^1/_2 - z$ and $x - {}^1/_2,{}^1/_2 - y,-z$, respectively, with respect to the unprimed molecule at x,y,z. It can be concluded that the difference (~10 ppm) in the tensor component along the corresponding C=O bond of the C4 and C6 nuclei is brought about by the different intermolecular C=O- - -H—C interactions. In fact, it has been pointed out[9] that intermolecular hydrogen bonding brings a large downfield shift to the tensor component along the C=O bond in the carbonyl carbon nucleus in **2**. Kempf et al.[30] have noted that the magnitudes of the tensor component along a C=O bond can vary widely for different carbonyl carbon nuclei.

Table IV. Comparison of "Local" Configurations around the Two Ester Carbon Nuclei (C4 and C6) in **1**[a]

	C4			C6		
	ref 5	ref 6	av	ref 5	ref 6	av
Intramolecular Angles (deg)						
O′-C-O*	118.9	118.6	118.8	119.2	119.6	119.4
O*-C-C5	124.8	125.1	125.0	125.6	124.4	125.0
O′-C-C5	116.3	116.4	116.4	115.2	116.0	115.6
Bond Lenghts (Å)						
O′-C	1.346	1.336	1.341	1.358	1.341	1.350
O*-C	1.199	1.200	1.200	1.187	1.192	1.190
C5-C	1.490	1.487	1.489	1.498	1.488	1.493
Intermolecular C=O- - -H—C5 Configurations						
Distance (Å)						
O- - -H	2.80	2.76	2.78	2.49	2.51	2.50
Angle (deg)						
O- - -H—C	92.6	96.0	94.3	130.1	128.0	129.1

[a] O* and O′ denote the corresponding carbonyl and ester oxygen nuclei, respectively.

Molecular Motion in Solid Meldrum's Acid (1). In this section, we investigate the possibility of an alternation of the intermolecular C=O- - -H—C configurations in **1** by using a one-dimensional exchange NMR experiment for the two ^{13}C resonances of the ester carbon nuclei. The 1D-exchange NMR technique applied here is described in detail in ref 11; the conventional pulse sequence applied for the 2D-exchange NMR experiments of a dilute spin in solids[21] is employed with special settings of the ^{13}C transmitter as the on-resonance frequency to one of the two ester carbon signals and the evolution time to satisfy $t_1 = 1/(4\Delta)$ where Δ is the off-resonance frequency in Hz of the other ester carbon signal. The resulting 1D-exchange NMR spectrum corresponds exactly to a slice of a 2D-exchange NMR spectrum, passing through one diagonal-peak and one cross-peak.

Under certain assumptions, the magnetizations corresponding to a diagonal-peak, M_D, and a cross-peak, M_C, can be written as[11]

$$M_D = -\exp(-t_1/T_2)\{\tfrac{1}{2}\exp(-\tau_m/T_1)[1 + \exp(-k\tau_m)]\}\mathrm{Tr}\{I_y^2\} \tag{3}$$

and

$$M_C = -\exp(-t_1/T_2)\{\tfrac{1}{2}\exp(-\tau_m/T_1)[1 - \exp(-k\tau_m)]\}\mathrm{Tr}\{I_y^2\} \tag{4}$$

where τ_m is the duration time for the mixing period when the exchange takes place with a rate constant k, T_2 is the dephasing time during the evolution period, and T_1 is the carbon spin–lattice relaxation time during the mixing period. A plot of $\ln[(1 + r)/(1 - r)]$ vs. τ_m yields k as the slope, where r is the ratio of the intensities of a diagonal-peak and a cross-peak, $r = M_C/M_D$.

The 1D-exchange NMR technique was used to investigate the two signals of the two ester carbon nuclei (C4 and C6) when the static magnetic field is along the crystallographic c axis, at various temperatures. Figure 4 shows the 1D-exchange NMR spectra at 300 K with mixing times of (a) 1 s, (b) 50 s, and (c) 125 s.

---

(26) Sastry, D. L.; Takegoshi, K.; McDowell, C. A., to be published.

(27) Another choice of the tensor for the quaternary carbon nucleus (C2) is possible. In that alternative tensor, the σ_{22} axis is perpendicular to the O–C–O plane, and the σ_{11} axis lies along the bisector of the O–C–O angle.

(28) Pines, A.; Abramson, E. *J. Chem. Phys.* **1974**, *60*, 5130–5131.

(29) For example, see: Levy, G. C.; Lichter, R. L.; Nelson, G. L. *Carbon-13 Nuclear Magnetic Resonance Spectroscopy*, 2nd ed.; Wiley: New York, 1980; Chapter 5.

(30) Kempf, J.; Spiess, H. W.; Haeberlen, U.; Zimmermann, H. *Chem. Phys.* **1974**, *4*, 269–276.

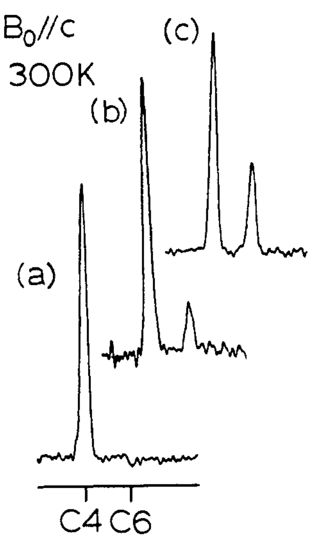

Figure 4. 1D-exchange NMR spectra for the C4 and C6 carbon nuclei in Meldrum's acid, when the static magnetic field is along the crystallographic *c* axis with mixing times of (a) 1, (b) 50, and (c) 125 s.

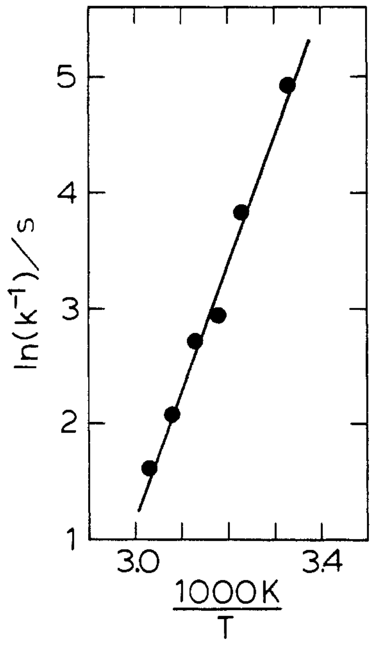

Figure 5. Arrhenius plot of the inverse of the exchange rate vs. the inverse of the temperature.

Chart I

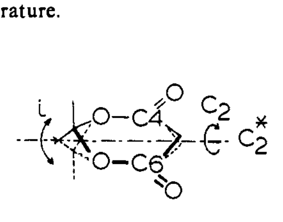

The cross-peaks obviously indicate that an exchange process takes place involving the C4 and C6 carbon nuclei in the solid state. Several similar 1D-experiments were performed at various temperatures, and the temperature dependence of the rate constant plotted in Figure 5 shows that the Arrhenius rate equation

$$k^{-1} = \tau_0 \exp(E_a/RT) \qquad (5)$$

is obeyed. The activation energy, E_a, and the correlation time at infinite temperature, τ_0, thus obtained are 91.4 ± 4.6 kJ/mol and 1.7×10^{-14} s^{-1} ($\ln(\tau_0) = -31.7 \pm 1.7$), respectively.

There are two possible mechanisms which can cause cross-peaks to be observed between the ^{13}C resonances of the C4 and C6 carbon; these are (i) molecular motion and (ii) ^{13}C spin-diffusion. We postulate that in Meldrum's acid, a possible molecular motion is a 180° rotation of a molecule (C_2 in Chart I) around a pseudo-C_2 axis (C_2* in Chart I) plus a "ring inversion" process[25] (*i* in Chart I), i.e., one which results in an interchange of the spatial positions of the C4 and C6 nuclei in the lattice. This composite molecular motion also involves an alternation of the intermolecular C=O--H—C configurations at the C4 and C6 nuclei. The ring inversion–rotation process which we postulate involves spatial interchange of the two methyl carbon nuclei (C21 and C22); thus, exchange NMR studies of the two methyl resonance lines could possibly provide supporting evidence for the mechanism of the molecular motion mentioned above. Unfortunately, the spin–lattice relaxation times, T_1, of the two methyl carbon nuclei are quite short ($T_1 \sim$ a few 100 ms) compared to the value of τ_m required to detect the molecular motion ($\tau_m \sim 10$ s) at any crystal orientation. Thus, neither cross-peaks nor diagonal-peaks could be observed in the 1D-exchange NMR spectrum of the two methyl signals.

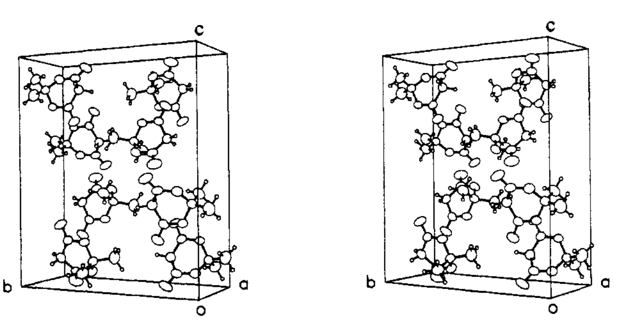

Figure 6. Stereoscopic drawing of molecular packing of Meldrum's acid in the unit cell of the crystal. *a*, *b*, and *c* denote three crystallographic axes.

Our experiments do not enable us to decide if the first event in the molecular motion is the "ring inversion" followed by the 180° rotation about the pseudo-C_2 axis, or vice versa. We prefer to regard these sequences to be parts of a concerted motion. It is clear that both components are necessary to maintain the crystal symmetry, otherwise defects would be introduced into the crystal lattice (Figure 6). The ring inversion–rotation molecular motion differs from and is more complex than the various ring flip processes which have been found to occur in many molecular solids and which have been studied in detail by NMR.[31] In solution, activation free energies for a ring inversion process in some 1,3-dioxane derivatives were determined to be about 40 kJ/mol by NMR methods.[32] The large activation energy which we find is attributed to the barrier to the ring inversion–rotation of a molecule around the C_2* axis in the crystal. It is noteworthy that proton exchange in solid tropolone studied by a similar NMR technique[8] yielded an activation energy of 110.9 kJ/mol. To explain this large value it was postulated that when a proton moves intramolecularly from a hydroxyl site to a carbonyl site in solid tropolone, simultaneously there is an out-of-plane molecular rotation which restores the carbonyl and hydroxyl carbons to their proper lattice positions. The large anisotropic thermal parameters observed in the X-ray crystallographic study of Meldrum's acid (Figure 1 of ref 5) are worthy of note. Frequently these have been associated with the presence of molecular motion, and it seems reasonable

---

(31) (a) Mansfield, M.; Boyd, R. H. *J. Polym. Sci.* **1978**, *16*, 1227–1252. (b) Kinsey, R. A.; Kintanar, A.; Oldfield, E. *J. Biol. Chem.* **1981**, *256*, 9028–9036. (c) Gall, C. M.; DiVerdi, J. A.; Opella, S. J. *J. Am. Chem. Soc.* **1981**, *103*, 5039–5043. (d) Rice, D. M.; Wittebort, R. J.; Griffin, R. G.; Meirovitch, E.; Stimson, E. R.; Meinwald, Y. C.; Freed, J. H.; Scheraga, H. A. *J. Am. Chem. Soc.* **1981**, *103*, 7709–7710. (e) Rice, D. M.; Blume, A.; Herzfeld, J.; Wittebord, R. J.; Huang, T. H.; DasGupta, S. K.; Griffin, R. G. *Biomol. Stereodyn.* **1981**, 255–270. (f) Spiess, H. W. *Colloid Polym. Sci.* **1983**, *261*, 193–209. (g) Schaefer, J.; Stejskal, E. O.; McKay, R. A.; Dixon, W. T. *J. Magn. Reson.* **1984**, *57*, 85–92; *Macromolecules* **1984**, *17*, 1479–1489. (h) Frey, M. H.; DiVerdi, J. A.; Opella, S. J. *J. Am. Chem. Soc.* **1985**, *107*, 7311–7315 and references cited therein.

(32) For a review, see: Anet, F. A. L.; Anet, R. *Dynamic Nuclear Magnetic Spectroscopy*; Jackman, L. M., Cotton, F. A., Eds.; Academic: New York, 1975; Table X.

to think that is perhaps part of their cause in this compound.

As is well-known ^{13}C spin-diffusion occurs by a "flip-flop" process of the ^{13}C spins governed by the term $(S_+S_- + S_-S_+)$ in the ^{13}C–^{13}C homonuclear dipolar interaction Hamiltonian.[33] Since this "flip-flop" process is an energy-conserving one by itself, it is clear that ^{13}C spin-diffusion is independent of temperature unless the efficiency of the process is enhanced by rotational or translational diffusion when it will be temperature dependent.[34] We performed similar 1D exchange NMR experiments to see if ^{13}C spin-diffusion occurred between the C2 and C6 carbon nuclei at room temperature when the static magnetic field is along the crystallographic *c* axis.[35] No cross-peaks larger than the background were observed with mixing times up to 100 s. Thus if spin-diffusion occurs in this case the rate must be less than the spin–lattice relaxation. Experiments using the combined techniques of 2D-exchange NMR and CP–MAS showed that cross-peaks due to ^{13}C spin-diffusion between three chemically inequivalent carbon nuclei in 1,4-dimethoxybenzene were observed with a mixing time of 90 s.[21] We now discuss why ^{13}C spin-diffusion is inefficient in Meldrum's acid.

The transition probability, W_{ij}, for ^{13}C spin-diffusion between a pair of carbon nuclei can be written as[33,36–38] $W_{ij} = (\pi/2)\omega_{ij}^2 f_{ij}(0)P(i,j)$. In this equation, $\omega_{ij} = (\gamma_c 2\hbar/2r_{ij}^3)(1 - 3\cos^2\theta_{ij})$, γ_c is the gyromagnetic ratio of a ^{13}C spin, r_{ij} is the distance between two carbon nuclei, θ_{ij} is the angle between the carbon–carbon vector and the static magnetic field, $f_{ij}(0)$ denotes the overlap of two ^{13}C resonances, and $P(i,j)$ is the probability of finding two ^{13}C nuclei in the configuration described above. At natural abundance in organic compounds ^{13}C is a dilute nucleus (natural abundance is 1.1%); one can therefore assume that any ^{13}C spin-diffusion occuring will be intermolecular. In Meldrum's acid, the factors determining ^{13}C spin-diffusion, such as P, r, and $f_{ij}(0)$, are quite unfavorable. This can be shown by comparison with 1,4-dimethoxybenzene.[21] In this latter compound, the closest intermolecular carbon–carbon distance is 3.54 Å, for a quaternary carbon (C1) and a ring carbon (C2) in the molecules related by the lattice coordinates x,y,z and $^1/_2 - x, ^1/_2 + y, z$, respectively.[39] In Meldrum's acid, the closest intermolecular distance for the C2, C4, C5, and C6 nuclei is 3.80 Å for C4 and C5 in molecules related by the lattice coordinates x,y,z and $^1/_2 + x, y, ^1/_2 - z$, respectively. At first glance, this difference in the intermolecular distances may not seem to be significant; however, since W_{ij} depends strongly on r_{ij}, this difference leads to W(C1–C2 in 1,4-dimethoxybenzene)/W(C4–C5 in Meldrum's acid) $\simeq$ 0.65, assuming the other factors to be equal. The closest intermolecular distance for the C4 and C6 nuclei in Meldrum's acid is 4.01 Å, thus, the ^{13}C spin-diffusion between these two carbon nuclei is more inefficient. The $f_{ij}(0)$ value can also be assumed to be small for the quaternary carbon nuclei in Meldrum's acid (C2, C4, and C6), because the spectral overlap between two ^{13}C resonances is provided by a line broadening due to a ^{13}C–^{1}H heteronuclear dipolar interaction.[36,37] Since in Meldrum's acid any rotational and/or translational molecular diffusion must be negligible at room temperature, the possibility, $P(i,j)$, of finding two ^{13}C spins adjacent or reasonably close is also negligibly small. All these factors make the ^{13}C spin-diffusion process likely to be ineffective in Meldrum's acid. Thus, the observed cross-peaks can most reasonably be assigned to a motional exchange between the C4 and C6 carbon nuclei taking place by the mechanism depicted in Chart I.

Acknowledgment. We thank the National Sciences and Engineering Research Council of Canada for financial support to C. A. McDowell in aid of this work. We also thank S. V. Evans and J. Trotter for determining the crystallographic orientation of the crystals and for allowing us to use unpublished X-ray crystallographic study to analyze our data, and for permission to use Figure 6.

Registry No. 1, 2033-24-1.

---

(33) Abragam, A. *The Principles of Nuclear Magnetism*; Oxford University: London, 1961.

(34) Caravatti, P.; Deli, J. A.; Bodenhausen, G.; Ernst, R. R. *J. Am. Chem. Soc.* **1982**, *104*, 5506–5507.

(35) Since ^{13}C spin-diffusion may occur between any ^{13}C nuclei in organic molecules, one should take into account any ^{13}C magnetizations stored along the static magnetic field by the application of the first ^{13}C 90° pulse in the 1D-exchange NMR experiment (ref 8 and 11). In our case, the ^{13}C transmitter frequency is chosen to be on-resonance for the C2 carbon, and the evolution time is carefully chosen to produce equal amounts of ^{13}C longitudinal magnetization at the C4 and C5 sites in an antiparallel direction to each other. With this experimental arrangement, the magnetizations transferred from the C4 and C5 sites to the C2 site cancel each other, and only the magnetization from the C6 site is observed.

(36) Bronniman, C. E.; Szeverenyi, N. M.; Maciel, G. E. *J. Chem. Phys.* **1983**, *79*, 3694–3700.

(37) Suter, D.; Ernst, R. R. *Phys. Rev.* **1982**, *B25*, 6038–6041.

(38) VanderHart, D. L.; Garroway, A. N. *J. Chem. Phys.* **1979**, *71*, 2773–2787.

(39) Goodwin, T. H.; Przybylska, M.; Robertson, J. M. *Acta Crystallogr.* **1950**, *3*, 279–284.